Respiratory Physiology & Neurobiology 268 (2019) 103252

Contents lists available at ScienceDirect

Respiratory Physiology & Neurobiology

journal homepage: www.elsevier.com/locate/resphysiol

Paeonol protects mitochondrial injury and prevents pulmonary vascular remodeling in hypoxia

Dapeng Wang[a], Yali Du[b], Hongyang Xu[a], Hong Pan[a], Ruilan Wang[c,*]

[a] Department of Intensive Medicine, The Affiliated Wuxi People's Hospital of Nanjing Medical University, Wuxi, Jiangsu, China
[b] Department of Obstetrics and Gynecology, The Affiliated Wuxi People's Hospital of Nanjing Medical University, Wuxi, Jiangsu, China
[c] Department of Critical Care Medicine, Shanghai General Hospital of Nanjing Medical University, Shanghai, China

ARTICLE INFO

Keywords:
Pulmonary artery smooth muscle cells
Mitochondria
Paeonol
Peroxisome proliferator-activated receptor-gamma co-activator 1α
Apoptosis

ABSTRACT

Mitochondrial injury of pulmonary artery smooth muscle cells (PASMCs) is an important stage in the development of pulmonary arterial hypertension (PAH). Recent studies revealed that Paeonol exerts anti-proliferative effects on vascular smooth muscle cells. However, whether Paeonol is directly involved in mitochondrial injury related to PAH remains unknown. Here, we found that hypoxia-induced mitochondrial injury in vivo was alleviated in the presence of Paeonol. Hypoxia mediated the mitochondrial injuries in PASMCs in vitro, including decreased ATP generation, morphological alterations, mitochondrial polarization and increased reactive oxygen species production, which were suppressed by Paeonol. Our results also indicated that the expression of peroxisome proliferator-activated receptor-gamma coactivator 1α (PGC-1α) was regulated by Paeonol. Paeonol caused significant alterations in mitochondrion-dependent apoptosis through PGC-1α in PASMCs. Taken together, these results provide the first evidence confirming the protective effect of Paeonol in mediating mitochondrial injury under hypoxia and elucidating the necessary role of PGC-1α in the effects of Paeonol in inducing PASMC apoptosis.

1. Introduction

Pulmonary arterial hypertension (PAH) involves a group of severe functional and structural changes in the pulmonary vasculature, including the accumulation of extracellular matrix and excessive proliferation and resistance to the apoptosis of pulmonary artery smooth muscle cells (PASMCs), pulmonary artery endothelial cells (PAECs) and adventitial fibroblasts leading to thickening of pulmonary arterioles (Boucherat et al., 2018; Humbert et al., 2019; Kovacs et al., 2019). PASMCs from animal models of pulmonary hypertension and human tissues with PAH are more hyperproliferative and resistant to apoptosis than normal PASMCs which are likely the major factors leading to pulmonary arterial medial hypertrophy in pulmonary vascular remodeling processes (Dai et al., 2018). However, the mechanisms underlying this aberrant apoptosis resistance in most forms of PAH remain unclear.

Paeonol (2′-hydroxy-4′-methoxyacetophenone, $C_9H_{10}O_3$) is a natural phenolic compound with bioactive constituents isolated from Cortex Moutan (Lau et al., 2007). Paeonol has been found to regulate a wide range of fundamental pharmacological activities such as anti-inflammatory, anti-atherosclerotic, anti-platelet, anti-oxidant, anti-diabetic, and anti-tumor activities (Liu et al., 2014; Lu et al., 2018). Paeonol induces gastric cancer cell apoptosis by downregulating epidermal growth factor receptor 2 (ERBB2) and inhibiting the nuclear factor kappa light chain enhancer of activated B cells (NF-κB) signaling pathway (Fu et al., 2018). Paeonol also attenuates lipopolysaccharide (LPS) -induced dysfunction in human endothelial cells by inhibiting bone morphogenic protein 4 (BMP4) and toll-like receptor 4 (TLR4) signaling (Choy et al., 2018). Additionally, Paeonol prevents cigarette smoke and bleomycin-induced pulmonary inflammation and fibrosis (Liu et al., 2017, 2014). Despite these pharmacological findings, the possible role of Paeonol in regulating PASMC apoptosis as related to PAH has yet to be elucidated.

Mitochondria have retained their own genome and possess autonomous protein synthesis machinery (Apostolova and Victor, 2015). The mitochondrion is believed to participate in crucial cell physiology functions including bioenergetics, metabolic pathways, Ca^{2+} homeostasis, reactive oxygen species (ROS) production, autophagy and apoptosis (Boengler et al., 2017; Brookes et al., 2002). Abnormalities in mitochondria are often observed in the pathophysiology of human diseases such as cancer, cardio-pulmonary system and neurodegenerative disease (Picard et al., 2016). One of the main regulators of

* Corresponding author at: 100 Haining Road, Hongkou District, Shanghai, China.
E-mail address: wangyusun@hotmail.com (R. Wang).

https://doi.org/10.1016/j.resp.2019.103252
Received 16 April 2019; Received in revised form 6 July 2019; Accepted 7 July 2019
Available online 10 July 2019
1569-9048/

mitochondrial homeostasis, including oxidative stress and energy metabolism, is peroxisome proliferator-activated receptor gamma coactivator 1-alpha (PGC-1α) (Kaminski et al., 2019; LeBleu et al., 2014). PGC-1α is a transcriptional coactivator that is highly expressed in the mitochondria and governs the expression of nuclear-encoded mitochondrial genes (Hock and Kralli, 2009). The influence of PGC-1α on mitochondrial biogenesis in multiple cancers, such as prostate cancer, hepatocarcinoma, melanoma and colon cancer has been recently demonstrated (LeBleu et al., 2014; Luo et al., 2019; Piccinin et al., 2018). In addition, PGC-1α has been shown to be related to neurodegenerative disorders, and a lack of PGC-1α is linked to the acceleration of Huntington's and Parkinson's disease progression (Nierenberg et al., 2018).

In PAH, mitochondrial dysfunction normally results in pathologic changes in PASMCs (Marsboom et al., 2012). The abnormal expression of mitochondrial proteins including dynamin-related protein 1 (Drp1), mitofusin 1 (Mfn1) and mitofusin 2 (Mfn2) is mechanistically related to the PASMC proliferation-apoptosis imbalance in PAH (Ma et al., 2017; Ryan et al., 2013). Although mitochondrial structure and function are involved in pulmonary vascular remodeling processes, to our knowledge, there have been no studies conducted to date evaluating the role of Paeonol in mitochondrial dysfunction with respect to PGC-1α in models of PAH. The linkage between Paeonol, PGC-1α, and PASMC apoptosis requires futher study.

Herein, we hypothesize that mitochondrial dysfunction increases under hypoxia which is responsible for the apoptosis resistance of PASMCs. The current study confirmes this notion and showes that Paeonol alleviates mitochondrial injury under hypoxic conditions and stimulates PASMC apoptosis to reverse experimental PAH through PGC-1α.

2. Material and methods

2.1. Animals

Adult male Sprague-Dawley (SD) rats (180–200 g) were from the Experimental Animal Center of The Affiliated Wuxi People's Hospital of Nanjing Medical University, the animal study protocol was approved by the Institutional Animal Care and Use Committee (IACUC) of Nanjing Medical University. All experimental procedures in animals were carried out and conducted incompliance with National Institutes of Health guide for the care and use of Laboratory animals (NIH Publications No. 8023, revised 1978).

2.2. Chronic hypoxia-induced PAH rats model

SD rats were exposed to 10% oxygen in a ventilated chamber for 21 days. The rats were randomly divided into three groups, Control + saline, Hypoxia + saline and Hypoxia + Paeonol. Paeonol (purity, ≥98.0%) was from Sigma (Sigma, USA). The rats received daily treatment with Paeonol (100 mg/kg/d) or saline (vehicle control) by gastric gavage from hypoxic day 10 to day 21 (Zhang et al., 2018; Li et al., 2016). Animals were given ad libitum access to food and water at a temperature of 21 ± 2 °C with a 12 h light/dark cycle.

2.3. Histological analysis and right ventricular (RV) hypertrophy measurements

At the end of the treatment protocol, the animals were anesthetized with intraperitoneally injected pentobarbital. The thoraxes of the animals were opened, and the left lungs were collected and kept in 10% formalin solution, after which paraffin blocks were prepared. Paraffinembedded lung blocks were cut into 5-μm sections, which were stained with hematoxylin-eosin (H&E). Images of the tissues were visualized by using an Eclipse 600 Nikon microscope. Morphometric analysis was performed with Image Pro Plus 6.0. For RV hypertrophy measurements, hearts were excised, and the atria were removed. The RV-free wall was dissected, and each chamber was then weighed. The ratio of RV weight to left ventricular (LV) weight plus septum (RV/LV + S) was used as an index of RV hypertrophy.

2.4. Cell culture

The primary culture of rat pulmonary artery smooth muscle cells (PASMCs) was isolated from rat pulmonary arteries. The isolated pulmonary arteries were digested with 0.2% collagenase and 0.2% Bovine Serum Albumin in PBS solution for 2 h at 37 °C. The PASMCs were cultured in DMEM (Dulbecco's modified eagle's medium) with 10% fetal bovine serum (FBS; HyClone; GE Healthcare Life Sciences, Logan, UT, USA), 100 μg/ml streptomycin and 100 U/ml penicillin was utilized to incubate the cells under a humidified atmosphere with 5% CO_2 at 37 °C. For induction of hypoxia, cells were cultured in a hypoxia incubator (Thermo Fisher Scientific, Inc.) with 3% O_2, 5% CO_2 at 37 °C.

2.5. Small interfering RNA (siRNA) design and transfection

To silence the expression of the PGC-1α protein, PASMCs were transfected with siRNA according to the previously published protocol (Wang et al., 2018). The sense sequence of siRNA was designed and synthesized by GenePharma (Shanghai, China). Sequence of siRNA against PGC-1α is : 5′-CCGAGAAUUCAUGGAGCAATT-3′, and negative control (NC) sequence is : 5′-UUCUCCGAACGUGUCACGUTT-3′. We cultivated the PASMCs until they reached 60–70% confluence, at which time 2 μg of siRNA and 10 μl of Lipofectamine 2000 reagent (Thermo Fisher Scientific, Inc.) were diluted in serum-free Opti-MEM-1 medium and mixed together. Then, the admixture (siRNA/Transfection Reagent) was incubated for 20 min at room temperature and added directly to the cells. The transfection reagent was removed 4–6 h after siRNA treatment. After transfection, the cells were quiescent for 24 h and were used as required.

2.6. Cell viability assay

PASMCs were seeded in 96-well culture plates (approximately 5×10^3), and the cells were then treated with different agents. The cells were exposed to hypoxia (3% O_2). After 24 h of incubation at 37 °C, the cells were incubated with 20 μl/well 3-(4,5-dimethyl-2-thiazolyl)-2,5-diphenyl-2-H-tetrazolium bromide (MTT) (Sigma Chemical, USA) for 4 h at 37 °C. The medium was then removed, and DMSO (200 μl/well) was added to solubilize the precipitate for 10 min at room temperature. The absorbance was then measured at 490 nm by using a spectrophotometer.

2.7. Hoechst 33342 staining for apoptosis detection

PASMCs were cultured in a six-well culture cluster to 60–70% confluence. The cells were treated as indicated groups. After 24 h, the cells were stained with 10 mg/ml of Hoechst 33342 (Beyotime, China) at room temperature in the dark for 20 min. Cells were washed with PBS and evaluated using a fluorescence microscope. Cells with nuclear crenation and fractionation were defined as apoptotic cells.

2.8. Mitochondrial membrane potential assay

Cells were cultured in six-well plates. After the indicated treatments, the cells were incubated with an equal volume of a 5,5′,6,6′-Tetrachloro-1,1′,3,3′-tetraethyl-imidacarbocyanine iodide (JC-1) (Beyotime, China) staining solution (10 μg/ml) at 37 °C for 30 min and then washed with PBS. Images obtained by fluorescence microscopy were analyzed for green and red fluorescence. Mitochondrial depolarization was expressed as an increase in the intensity ratio of green/red fluorescence.

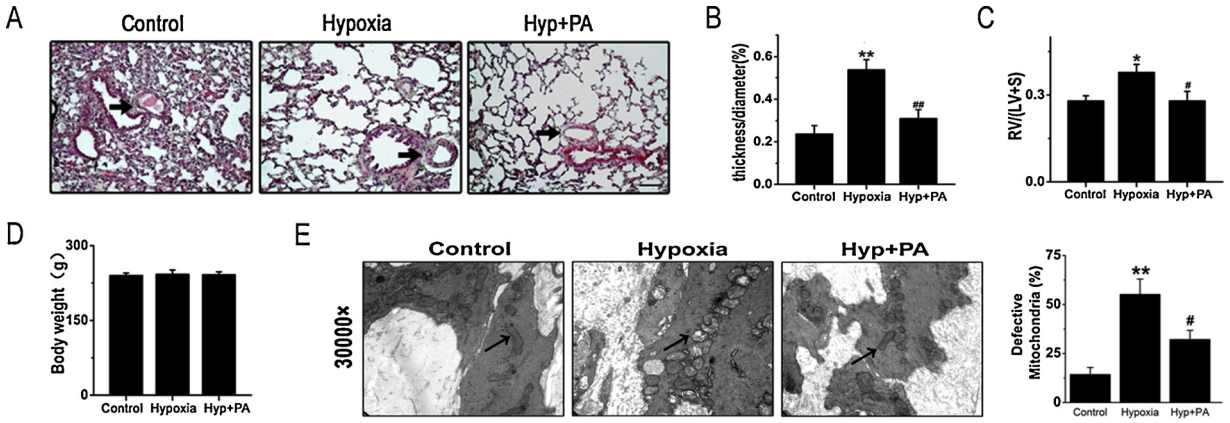

Fig. 1. Role of Paeonol in hypoxia-induced PAH.
A, Sections of lung tissues from rats exposed to normoxic or hypoxic conditions were identified using H&E staining. Scale bars are 100 μm. B, The summarized data represent the percentage of the medial thickness of the vessel wall. C, Ratio of the right ventricle to the left ventricle plus septum. Hypoxia significantly increased the ratio of the right ventricle compared with that in normoxic rats, which was partially reversed by the administration of Paeonol. D, Body weight of rats from the control, hypoxia, and hypoxia with Paeonol groups. E, The morphology of mitochondria in pulmonary arteries (PAs) was determined by transmission electron microscopy. Hyp, hypoxia; PA, Paeonol, All values are denoted as mean ± SEM. n = 6. $^{*}P < 0.05$, $^{**}P < 0.01$ compared with control. $^{\#}P < 0.05$, $^{\#\#}P < 0.01$ compared with hypoxia.

2.9. Flow cytometry analysis of cells apoptosis

Apoptosis rates were evaluated by flow cytometry using an Annexin V-fluorescein isothiocyanate (FITC) Kit (Beyotime, China) according to the manufacturer's protocols. Briefly, after the treatments, the cells were harvested and 195 μl of buffer, 15 μl of FITC -AnnexinV and 5 μl of propidium iodide (PI) were added, followed by incubation for 30 min in the dark at room temperature, and the percentage of apoptotic cells was immediately assessed using a flow cytometer.

2.10. Immunofluorescence

PASMCs were treated with different agents. Then, the cells were fixed with 4% paraformaldehyde for 20 min at room temperature. Next, the cells were permeabilized in 0.5% Triton X-100 on ice for 15 min, and washed in PBS 3 times. Immunofluorescence staining was performed by incubation with a PGC-1α antibody (1:100; Boster Biological Technology Co. Ltd, China) overnight at 4 °C, and followed by incubation with an Alexa Fluor 488 anti-rabbit IgG secondary antibody (1:100; Beyotime, China) at 37 °C for 1 h. The cells were next incubated with DAPI for nuclear staining at room temperature for 15 min. Microscopy analysis was performed with a fluorescence microscope.

2.11. Mitochondrial fragmentation and ROS measurements

PASMCs were treated with Paeonol (200 μM) and administrated under 3% oxygen exposure for 24 h. The cells were subsequently loaded with 20 μM Mitochondrial Superoxide Indicator (MitoSOX) Red (Santa Cruz, USA) for 30 min at 37 °C to measure the mitochondrial ROS. To measure the mitochondrial fragmentation, a photo activatable green fluorescent tracker, mitochondrial-tracker (Beyotime, China) was used. After washing three with PBS, the accumulation of ROS (red) and mitochondrial-tracker (green) was visualized using fluorescence microscope respectively.

2.12. Western blot analysis

Briefly, the cell lysates and pulmonary arteries were prepared using cell lysis buffer (Cell Signaling, Beverly, MA, USA). Equal amount of protein were separated by 8–12% SDS-PAGE and electro-transferred onto a polyvinylidene diuoride membrane (Millipore Corp., Bedford, MA). After being blocked with 5% nonfat dry milk for 1 h. Antibodies against PGC-1α (1:500), Caspase-3 (1:500; Boster Biological Techology Co. Ltd, China) B-cell lymphoma-2 (Bcl 2) (1:1000; Boster Biological Techology Co. Ltd, China) and β-actin (1:4000, Santa Cruz, USA) were used in this study. Membranes were incubated overnight at 4 °C. Blots were then incubated with horseradish peroxidase-conjugated secondary antibodies (Santa Cruz, USA) and enhanced by chemiluminescence reagents.

2.13. Determination of adenosine triphosphate (ATP) levels

The level of ATP in PASMCs was determined using the ATP Bioluminescence Assay Kit (Beyotime, China). PASMCs were treated with different agents, the level of ATP was determined by mixing 50 μl of the supernatant with 50 μl of luciferase reagent, the emitted light was measured using a microplate luminometer.

2.14. Transmission electron microscopy (TEM) analysis

For TEM morphological analysis, samples were fixed for 4 h in 2% glutaraldehyde and post-fixed by 1% osmium tetroxide. After gradually dehydrated in ethano, samples were embedded in Epon-Araldite resin. Thin sections were stained with uranyl acetate and lead citrate. The Zeiss EM902 electron microscope was utilized to observe the mitochondria.

2.15. Statistical analysis

The data were expressed as means ± SEM. One-way ANOVA analysis followed by Dunnett's test where appropriate was performed by GraphPad Prism 5.0. Multiple comparison between the groups was performed using Student-Newman-Keul's post hoc test. P-value < 0.05 was defined as statistically significant.

3. Results

3.1. Paeonol prevents pulmonary arterial medial hypertrophy and mitochondrial damage from hypoxia in vivo

Morphometric analysis of the pulmonary vasculature through hematoxylin and eosin (H&E) staining demonstrated that pulmonary vascular walls in lung tissue sections from rats subjected to hypoxia were significantly increased compared with those from control rats.

This increase was partially blocked by treatment with Paeonol (Fig. 1A-B). The ratio of right ventricle (RV) weight to left ventricular (LV) weight plus septum (RV/LV + S) was used as an index of RV hypertrophy. The RV/LV + S ratio was significantly increased in the hypoxia group compared with that in the control rats, and Paeonol significantly reversed the augment of RV/LV + S ratio induced by hypoxia (Fig. 1C). We observed no changes in body weight of the rats with or without Paeonol treatment (Fig. 1D). More importantly, the mitochondrial morphological changes inpulmonary arteries (PAs) were determined by transmission electron microscopy (TEM) in the PAH models. Hypoxia treatment led to the occurrence of mitochondrial damage as revealed by swelling, medullar and vacuolar degeneration, which was attenuated by Paeonol treatment (Fig. 1E).

3.2. Paeonol stimulates mitochondrion-dependent apoptosis of PASMCs under hypoxic conditions

To explore the role of Paeonol in the apoptotic effect on PASMCs under hypoxia, cell viability was determined. First, we determined the range of Paeonol concentration in vitro according to previous reports (Zhang et al., 2018). The increase in cell viability under hypoxic conditions was partly reversed by Paeonol treatment at 100 and 200 μM (Fig. 2A). Paeonol at a concentration of 200 μM was considered to be the more efficient dose and was used in the following experiments. The morphology of the abnormal nuclear contents (crenation, condensation and fractionation) in different groups is shown in Fig. 2B. Hypoxia treatment attenuated nuclear deformation which was partly reversed by Paeonol. Flow cytometry analysis with Annexin V and propidium iodide (PI) staining in cells revealed that the production of apoptotic cells was decreased in the presence of hypoxia, and this inhibitory effect on cell apoptosis was abolished by Paeonol (Fig. 2C). The JC-1 probe was used to analyze the changes in mitochondrial membrane potential. When the mitochondrial membrane potential is damaged in apoptotic cells, JC-1 retains its monomeric form and exhibits green fluoresce. PASMCs cultured in hypoxic conditions presented a significant increase in the mitochondrial membrane potential, as indicated by a notable decrease in the ratio of green/red fluorescence versus the control. Paeonol treatment increased the mitochondrial depolarization (Fig. 2D). Bcl 2 and caspase 3, which are closely associated with mitochondrial function and cell apoptosis, were examined in this study. A dramatic increase in Bcl 2 expression was observed in PASMCs under hypoxia, but this alteration was attenuated by applying Paeonol (Fig. 2E). Meanwhile, hypoxia inhibited the activation of caspase 3 compared with that in control, while Paeonol treatment increased its expression (Fig. 2F). These results show that Paeonol inhibits the proliferation and stimulates the apoptosis of PASMCs under hypoxia via the mitochondrial pathway.

3.3. Paeonol protects against mitochondrial injury due to hypoxia in vitro

To further confirm the significance of Paeonol for mitochondrial function, the ATP generation, mitochondrial morphology and mitochondrial oxidative stress of PASMCs were measured. There was a significant decrease in the ATP generation of PASMCs under hypoxia, suggesting mitochondrial dysfunction, which was recovered by Paeonol treatment (Fig. 3A). Mitochondrial morphology was assayed by using a Mito Traker green fluorescent probe. Hypoxia increased mitochondrial fragmentation, as visualized on the basis of fewer elongated tubules and short fragments of mitochondria in PASMCs, which was reversed by Paeonol (Fig. 3B). We then performed MitoSOX Red staining to examine the effects of hypoxia on mitochondrial ROS generation. Fig. 3C shows the increase in mitochondrial-derived ROS production in PASMCs in response to hypoxia, whereas Paeonol inhibited this effect. Moreover,

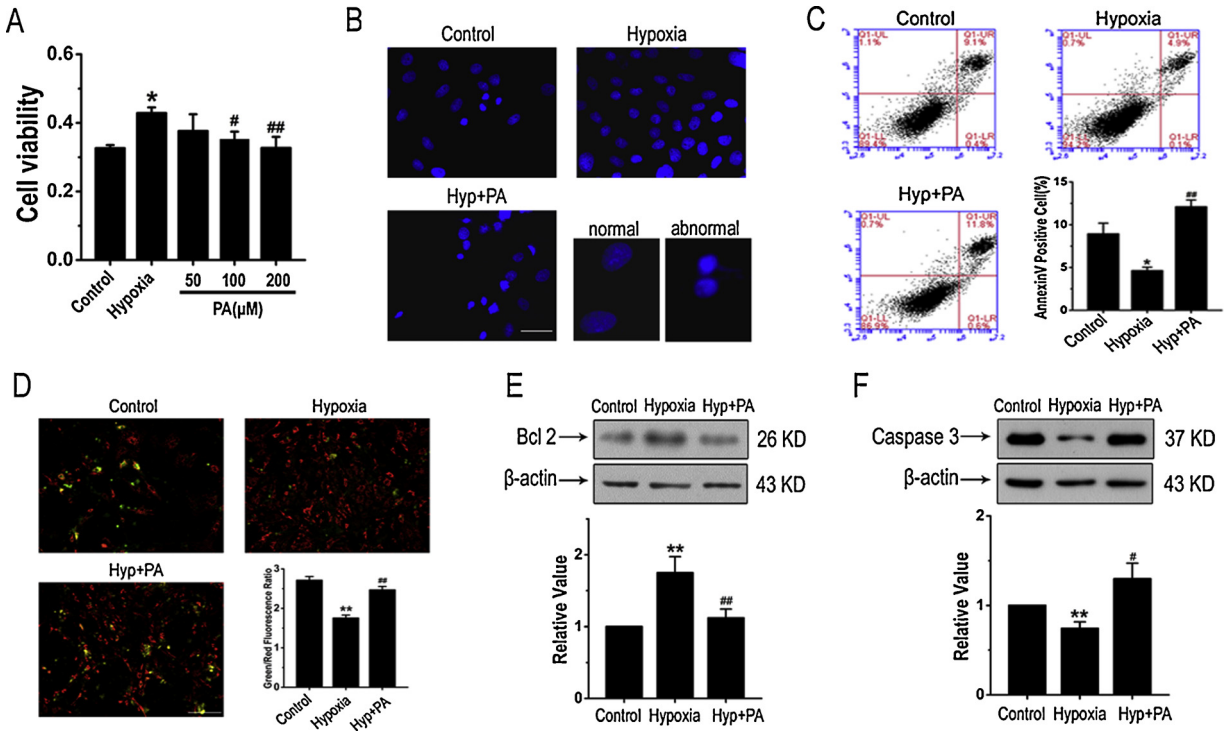

Fig. 2. Effects of Paeonol on cell apoptosis in PASMCs.
A, Cell viability was detected with MTT after adding Paeonol to PASMCs. B, Paeonol induced nuclear deformation and chromatin condensation under hypoxia; scale bars are 100 μm. C, Paeonol increased cell apoptosis as determined by flow cytometry. D, Representative photographs of JC-1 staining in different groups and the increase in the green to red fluorescence ratio, which is correlated with an increase in mitochondrial depolarization. Scale bars are 100 μm. E, The increase in the expression of Bcl 2 induced by hypoxia is partly inhibited by Paeonol. F, The decrease in the expression of capase 3 caused by hypoxia is inhibited by Paeonol. Hyp, hypoxia; PA, Paeonol, All values are denoted as mean ± SEM. n = 6. $^{*}P < 0.05$, $^{**}P < 0.01$ compared with control. $^{\#}P < 0.05$, $^{\#\#}P < 0.01$ compared with hypoxia.

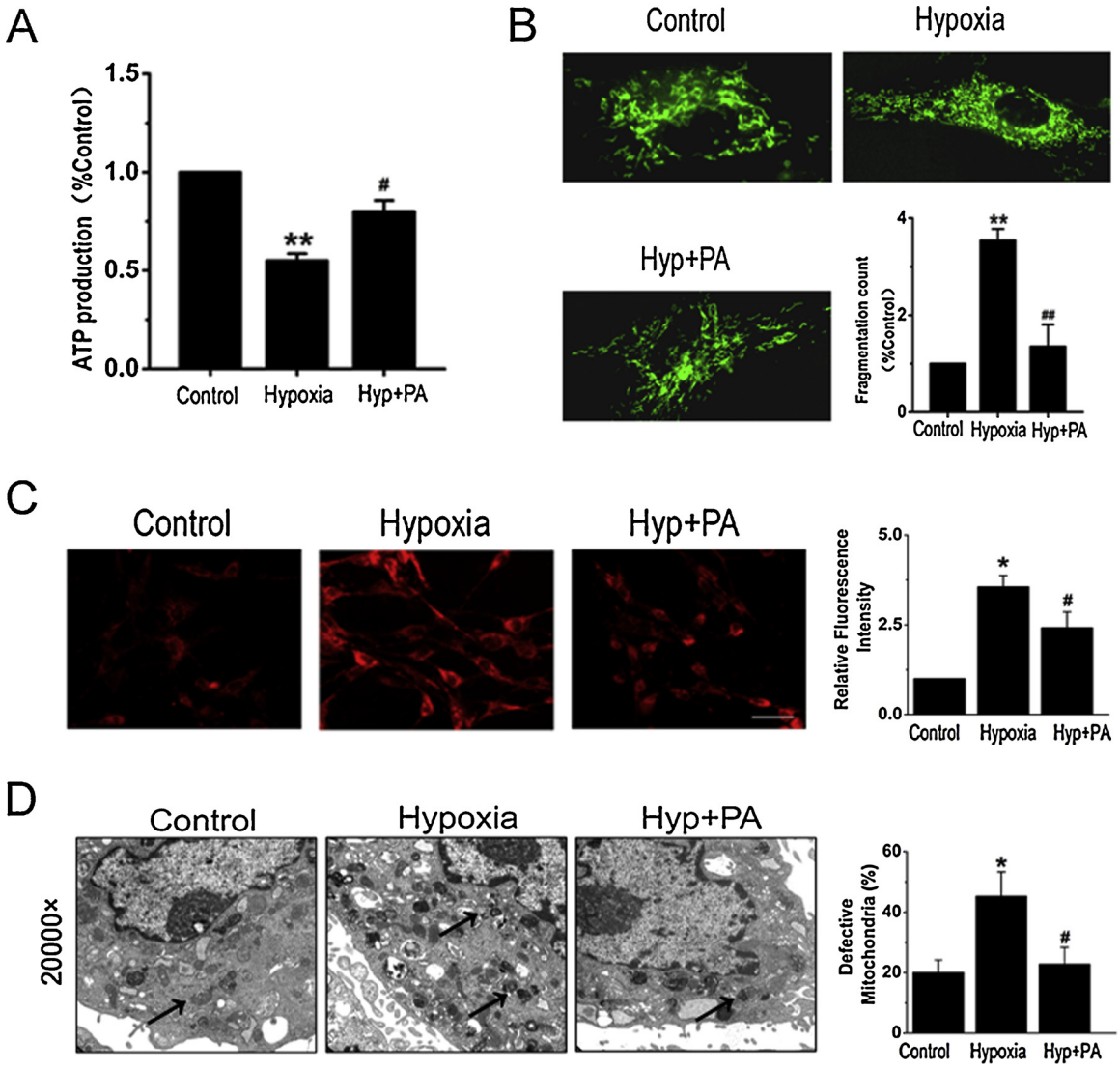

Fig. 3. Paeonol attenuated hypoxic mitochondrial damage in cultured PASMCs.
A, Paeonol recovered ATP generation under hypoxia. B, Images of mitochondrial morphology in PASMCs as determined by Mito-Tracker green staining. C, MitoSOX Red staining for mitochondrial ROS production, Scale bars are 50 μm. D, The morphology of mitochondria in cultured PASMCs treated with Paeonol under hypoxic conditions was determined by TEM. Hyp, hypoxia; PA, Paeonol, All values are denoted as mean ± SEM. n = 6. $^{**}P < 0.01$ compared with control. $^{\#}P < 0.05$, $^{\#\#}P < 0.01$ compared with hypoxia.

the morphology of mitochondria assayed by TEM showed vacuolar and developed medullary lesions of mitochondria under hypoxia, and these effects were diminished with Paeonol treatment (Fig. 3D).

3.4. PGC-1α could be induced by hypoxia and mediated by Paeonol

Previous studies have reported that PGC-1α is a central modulator of mitochondrial biogenesis and oxidative metabolism (Bost and Kaminski, 2019; Kelly and Scarpulla, 2004). To explore whether PGC-1α contributed to the regulation of mitochondrial functions by Paeonol, we first examined the effect of Paeonol on PGC-1α expression in pulmonary arteries and PASMCs. The results showed that hypoxia induced an increase in the expression of PGC-1α in pulmonary arteries and PASMCs and that the effect was reversed by Paeonol (Fig. 4A-B). Through immunofluorescent assays we observed that PGC-1α was mainly distributed in the cytosol and that hypoxia treatment increased the expression of PGC-1α compared with the controls. The effect of hypoxia was greatly inhibited by Paeonol (Fig. 4C).

3.5. Paeonol stimulates PASMC apoptosis in a PGC-1α-dependent manner

We next investigated the involvement of PGC-1α in the mitochondrion-dependent apoptosis of PASMCs in response to hypoxia. The expression of the PGC-1α protein was inhibited by transfecting the specific siPGC-1α sequence into PASMCs compared with the negative control (NC) (Fig. 5A). Then the cell viability assay was performed. The cell viability of PASMCs was found to be increased under hypoxia, and this increase was eliminated by PGC-1α silencing. After inhibiting PGC-1α, cell growth did not further decrease with the addition of exogenous Paeonol (Fig. 5B). Normal and abnormal (crenation, condensation and fractionation) nuclei are indicated as labeled in Fig. 5C. Paeonol or siPGC-1α treatment alone promoted nuclear deformation compared with hypoxia treatment respectively, and no further changes were observed in the Paeonol plus siPGC-1α group. Similar effects of Paeonol and siPGC-1α on PASMC apoptosis were identified by Flow cytomety analysis with Annexin V and PI staining (Fig. 5D). Loss of the mitochondrial membrane potential is an important indicator of cell apoptosis. As shown in Fig. 5E, hypoxia-inhibited mitochondrial depolarization as indicated by reduced ratios of green/red fluorescence.

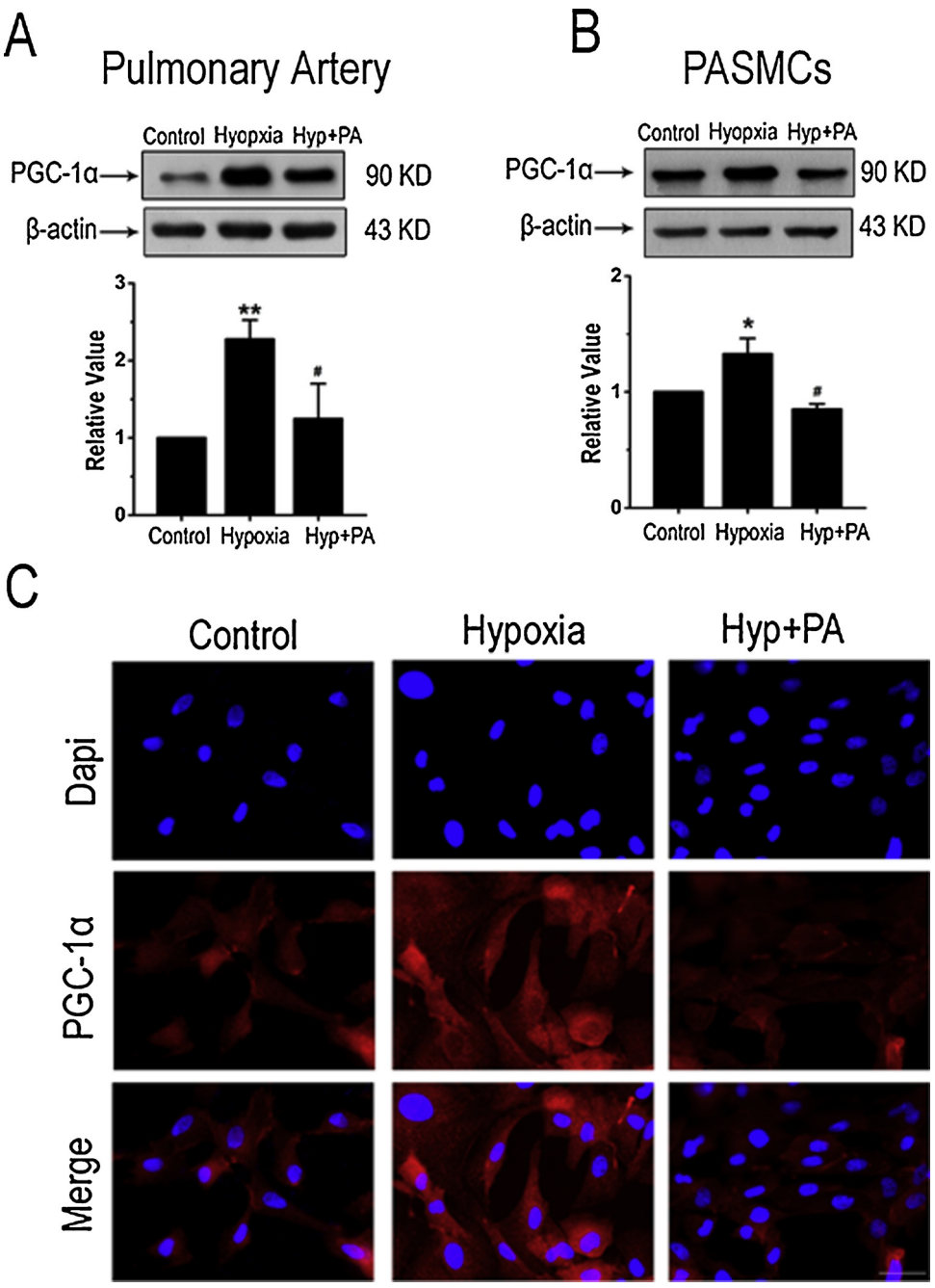

Fig. 4. Hypoxia increased the expression of PGC-1α in cultured PASMCs.
A-B, PGC-1α levels were increased in both hypoxic pulmonary arteries and PASMCs compared with the controls, which was inhibited by Paeonol. C, PASMCs were fixed and stained with anti-PGC-1α (red) and with DAPI (blue) to label the nucleus. Scale bars are 100 μm. Hyp, hypoxia; PA, Paeonol, All values are denoted as mean ± SEM. n = 6. $^{*}P < 0.05$, $^{**}P < 0.01$ compared with control. $^{\#}P < 0.05$ compared with hypoxia.

Treatment with Paeonol or siPGC-1α prevented the increase of mitochondrial potential caused by hypoxia, and no further changes were observed in paeonol-treated cells in which PGC-1α activity was blocked via RNA interference under hypoxic conditions. Bcl 2 is an important anti-apoptotic protein localized on mitochondrial membrane and is closely associated with mitochondrial function. We found that hypoxia upregulated Bcl 2 expression in PASMCs, while Paeonol / siPGC-1α alone decreased the expression of Bcl 2 to a similar extent as Paeonol together with siPGC-1α treatment (Fig. 5F). Furthermore, treatment with Paeonol / siPGC-1α resulted in an increased expression of caspase 3 compared with hypoxia, a similar result was acquired in the siPGC-1α plus Paeonol group (Fig. 5G). These results indicate that Paeonol stimulates the mitochondrion-dependent apoptosis of PASMCs through the PGC-1α pathway under hypoxia.

4. Discussion

Although prostacyclin analogues, prostacyclin receptor agonists, phosphodiesterase type 5 inhibitors, guanylate cyclase stimulators and endothelin receptor antagonists are included in the treatment for PAH patients (Galie et al., 2019). Current medical therapy is limited to reverse the complex progressive increases in pulmonary vascular resistance and severe PAH remains debilitating and deadly (Galie et al., 2016). Further treatment escalation is required, and the identification and validation of new pathways, drugs and strategies for combination therapy are therefore mandatory. In the present study, we attempted to

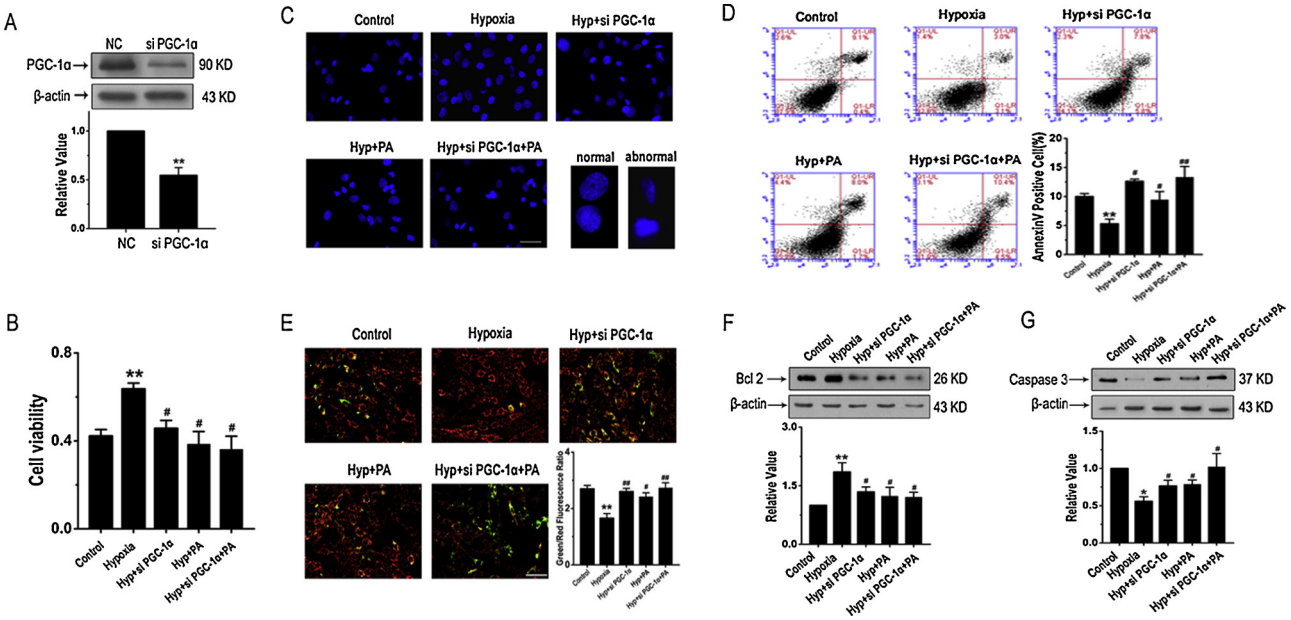

Fig. 5. PGC-1α was required for Paeonol-induced PASMC apoptosis under hypoxia.
A, The efficiency and specificity of siRNA directed against PGC-1α. B, The protective effect of hypoxia on cell viability was repressed by PGC-1α silencing. C, Cells were stained with Hoechst; abnormal (fractionation) and normal nuclei were labeled; and cells were imaged by fluorescent microscopy, Scale bars are 50 μm. D, Apoptosis analysis by flow cytometry showed that the decrease in apoptotic cells caused by hypoxia was increased by siPGC-1α. E, Representative photographs of cells stained with the JC-1 probe. Hypoxia attenuated mitochondrial depolarization in PASMCs, which was recovered by silencing PGC-1α. Scale bars are 100 μm. F–G, The effects of Paeonol and siPGC-1α on the expression of Bcl 2 and caspase 3. Hyp, hypoxia; PA, Paeonol, All values are denoted as mean ± SEM. n = 6. $^{*}P < 0.05$, $^{**}P < 0.01$ compared with control. $^{\#}P < 0.05$, $^{\#\#}P < 0.01$ compared with hypoxia.

explore the role of Paeonol in PASMC apoptosis and clarify the underlying mechanisms in vivo and in vitro.

The regulation of cell function by mitochondria is of great complexity and diversity, mitochondria depolarization is implicated in the regulation of cell apoptosis via the loss of mitochondrial membrane permeability and the release of cytochrome c (Cytc), second mitochondria-derived activator of caspases and apoptosis-inducing factor (AIF) from the matrix to the cytoplasm (Naoi et al., 2019). For example, in colorectal cancer SW480 cells, increases in mitochondrial elongation factor 1 (MIEF1)-induced mitochondrial outer potential deficiency and cellular ATP metabolism disorders participate in mitochondrial apoptosis initiation (Zhang et al., 2019). On the other hand, contrast to the classic theory, Marsboom et al. showed that increased dynamin-related protein 1 (Drp1) expression and activation reflects mitochondrial dysfunction resulting in hyperproliferative but not apoptotic diathesis of human PAH PASMCs (Marsboom et al., 2012). Similarly, Zhang et al. reported that increased mitochondrion-derived ROS (mROS) production was involved in PASMC apoptosis resistance induced by hypoxia (Zhang et al., 2016). Consistent with the above findings, in the present study mitochondrial damage including impaired ATP production, abnormal mitochondrial morphology and increased ROS production was increased by hypoxia. In addition, the JC-1 assay indicated that hypoxia treatment significantly increased the PASMC mitochondrial membrane potential by mitochondrial hyperpolarization which in turn promoted the expression of the apoptosis-inhibitory protein Bcl 2 to achieve its inhibition of cell apoptosis. Therefore, our results showed that hypoxia treatment was able to cause mitochondrial damage by contributing to the imbalance between cell apoptosis and proliferation, apoptosis resistance and increased proliferation in PASMCs ultimately leading to pulmonary vascular remodeling.

Accumulating evidence indicates that Paeonol exhibits various physiological properties relevant to the experimental treatment of respiratory system disease. Liu et al. determined that Paeonol attenuates cigarette smoke-induced lung inflammation by inhibiting ROS-sensitive inflammatory signaling pathways and interleukin-8 (Liu et al., 2014). Additionally, aminothiazole-paeonol derivatives provide an effective strategy for the treatment of acute lung injury (ALI) and acute respiratory distress syndrome (ARDS) induced by LPS (Fu et al., 2017). In hypoxic lungs, Paeonol has been reported to alleviate PASMC proliferation induced by chronic hypoxia by inhibiting extracellular regulated protein kinases (ERK 1/2) signaling pathway (Zhang et al., 2018). However, our knowledge about the mechanisms by which Paeonol causes hypoxic PAH is still incomplete. In the present study, we found that mitochondrial injuries in PASMCs including impaired ATP production, abnormal mitochondrial morphology and an increase in ROS induced by hypoxia are eliminated by Paeonol. Moreover, Paeonol stimulates the mitochondrion-dependent apoptosis of PASMCs and leads to relieved pulmonary arterial medial hypertrophy under hypoxia. To our knowledge, this is the first systematic study to associate Paeonol with mitochondrial homeostasis and cell apoptosis in PASMCs.

PGC-1α is a member of the peroxisome proliferator-activated receptor γ (PPARγ) coactivator family, which consists of PGC-1α (PPARGC1A), PGC-1β (PPARGC1B) and PRC (PPRC1) (Luo et al., 2016). PGC-1α has widespread functions in the human brain, neurons, hepatocytes, muscle and heart (Choi et al., 2014; Sawada et al., 2014). Researchers suggest that PGC-1α is a central regulator of mitochondrial biogenesis that can activate transcriptional factors such as nuclear respiratory factor 1 (NRF1) and mitochondria transcription factor A (TFAM) to improve mitochondrial biogenesis (Kelly and Scarpulla, 2004). Recent studies showed that activation of PGC-1α could reduce mitochondrial apoptosis in human sarcoma cell lines, and the inhibition of PGC-1α is causally related to hyperglycemia-induced vascular smooth muscle cell proliferation and migration (Onishi et al., 2014; Zhu et al., 2009). In pulmonary hypertension, PGC-1α protects against hypoxic endothelial cell injury by reducing oxidative stress and improving mitochondrial respiratory function (Ye et al., 2016). These results indicate that PGC-1α may act as a causal factor of the pathophysiologic process in cell apoptosis and is a potential therapeutic target for PAH. Our results reveal that PGC-1α is involved in the changes in cell viability, mitochondrial depolarization and Bcl 2 expression induced by

Paeonol in PASMCs. Additionally, PGC-1α mediates Paeonol-stimulated apoptosis through the mitochondrial pathway. The close relationship between mitochondrial functions and PGC-1α regulation in the pathological process in the pulmonary vasculature may provide combined therapeutic targets for hypoxic PAH.

5. Conclusions

Here, we demonstrate that Paeonol protects against mitochondrial injury from hypoxia both in vivo and in vitro, which is involved in hypoxia-induced pulmonary vascular remodeling. Moreover, we prove that Paeonol-mediated PASMC mitochondrial homeostasis and cell apoptosis are regulated by PGC-1α under hypoxic conditions.

Declaration of Competing interest

None.

Acknowledgement

This work was supported by the grants from National Natural Science Foundation of China (No. 81500039).

References

Apostolova, N., Victor, V.M., 2015. Molecular strategies for targeting antioxidants to mitochondria: therapeutic implications. Antioxid. Redox Signal. 22, 686–729.
Boengler, K., Kosiol, M., Mayr, M., Schulz, R., Rohrbach, S., 2017. Mitochondria and ageing: role in heart, skeletal muscle and adipose tissue. J. Cachexia Sarcopenia Muscle 8, 349–369.
Bost, F., Kaminski, L., 2019. The metabolic modulator PGC-1alpha in cancer. Am. J. Cancer Res. 9, 198–211.
Boucherat, O., Peterlini, T., Bourgeois, A., Nadeau, V., Breuils-Bonnet, S., Boilet-Molez, S., Potus, F., Meloche, J., Chabot, S., Lambert, C., Tremblay, E., Chae, Y.C., Altieri, D.C., Sutendra, G., Michelakis, E.D., Paulin, R., Provencher, S., Bonnet, S., 2018. Mitochondrial HSP90 accumulation promotes vascular remodeling in pulmonary arterial hypertension. Am. J. Respir. Crit. Care Med. 198, 90–103.
Brookes, P.S., Levonen, A.L., Shiva, S., Sarti, P., Darley-Usmar, V.M., 2002. Mitochondria: regulators of signal transduction by reactive oxygen and nitrogen species. Free Radic. Biol. Med. 33, 755–764.
Choi, J., Chandrasekaran, K., Inoue, T., Muragundla, A., Russell, J.W., 2014. PGC-1alpha regulation of mitochondrial degeneration in experimental diabetic neuropathy. Neurobiol. Dis. 64, 118–130.
Choy, K.W., Lau, Y.S., Murugan, D., Vanhoutte, P.M., Mustafa, M.R., 2018. Paeonol attenuates LPS-Induced endothelial dysfunction and apoptosis by inhibiting BMP4 and TLR4 signaling simultaneously but independently. J. Pharmacol. Exp. Ther. 364, 420–432.
Dai, J., Zhou, Q., Chen, J., Rexius-Hall, M.L., Rehman, J., Zhou, G., 2018. Alpha-enolase regulates the malignant phenotype of pulmonary artery smooth muscle cells via the AMPK-Akt pathway. Nat. Commun. 9, 3850.
Fu, J., Yu, L., Luo, J., Huo, R., Zhu, B., 2018. Paeonol induces the apoptosis of the SGC7901 gastric cancer cell line by downregulating ERBB2 and inhibiting the NFkappaB signaling pathway. Int. J. Mol. Med. 42, 1473–1483.
Fu, P.K., Yang, C.Y., Huang, S.C., Hung, Y.W., Jeng, K.C., Huang, Y.P., Chuang, H., Huang, N.C., Li, J.P., Hsu, M.H., Chen, J.K., 2017. Evaluation of LPS-Induced acute lung injury attenuation in rats by aminothiazole-paeonol derivatives. Molecules 22.
Galie, N., Channick, R.N., Frantz, R.P., Grunig, E., Jing, Z.C., Moiseeva, O., Preston, I.R., Pulido, T., Safdar, Z., Tamura, Y., McLaughlin, V.V., 2019. Risk stratification and medical therapy of pulmonary arterial hypertension. Eur. Respir. J. 53.
Galie, N., Humbert, M., Vachiery, J.L., Gibbs, S., Lang, I., Torbicki, A., Simonneau, G., Peacock, A., Vonk Noordegraaf, A., Beghetti, M., Ghofrani, A., Gomez Sanchez, M.A., Hansmann, G., Klepetko, W., Lancellotti, P., Matucci, M., McDonagh, T., Pierard, L.A., Trindade, P.T., Zompatori, M., Hoeper, M., Group, E.S.C.S.D., 2016. 2015 ESC/ERS guidelines for the diagnosis and treatment of pulmonary hypertension: the joint task force for the diagnosis and treatment of pulmonary hypertension of the european society of cardiology (ESC) and the european respiratory society (ERS): endorsed by: association for european paediatric and congenital cardiology (AEPC), international society for heart and lung transplantation (ISHLT). Eur. Heart J. 37, 67–119.
Hock, M.B., Kralli, A., 2009. Transcriptional control of mitochondrial biogenesis and function. Annu. Rev. Physiol. 71, 177–203.
Humbert, M., Guignabert, C., Bonnet, S., Dorfmuller, P., Klinger, J.R., Nicolls, M.R., Olschewski, A.J., Pullamsetti, S.S., Schermuly, R.T., Stenmark, K.R., Rabinovitch, M., 2019. Pathology and pathobiology of pulmonary hypertension: state of the art and research perspectives. Eur. Respir. J. 53.
Kaminski, L., Torrino, S., Dufies, M., Djabari, Z., Haider, R., Roustan, F.R., Jaune, E., Laurent, K., Nottet, N., Michiels, J.F., Gesson, M., Rocchi, S., Mazure, N.M., Durand, M., Tanti, J.F., Ambrosetti, D., Clavel, S., Ben-Sahra, I., Bost, F., 2019. PGC-1alpha inhibits polyamine synthesis to suppress prostate cancer aggressiveness. Cancer Res.
Kelly, D.P., Scarpulla, R.C., 2004. Transcriptional regulatory circuits controlling mitochondrial biogenesis and function. Genes Dev. 18, 357–368.
Kovacs, L., Cao, Y., Han, W., Meadows, L., Kovacs-Kasa, A., Kondrikov, D., Verin, A.D., Barman, S.A., Dong, Z., Huo, Y., Su, Y., 2019. PFKFB3 in smooth muscle promotes vascular remodeling in pulmonary arterial hypertension. Am. J. Respir. Crit. Care Med.
Lau, C.H., Chan, C.M., Chan, Y.W., Lau, K.M., Lau, T.W., Lam, F.C., Law, W.T., Che, C.T., Leung, P.C., Fung, K.P., Ho, Y.Y., Lau, C.B., 2007. Pharmacological investigations of the anti-diabetic effect of Cortex Moutan and its active component paeonol. Phytomedicine 14, 778–784.
LeBleu, V.S., O'Connell, J.T., Gonzalez Herrera, K.N., Wikman, H., Pantel, K., Haigis, M.C., de Carvalho, F.M., Damascena, A., Domingos Chinen, L.T., Rocha, R.M., Asara, J.M., Kalluri, R., 2014. PGC-1alpha mediates mitochondrial biogenesis and oxidative phosphorylation in cancer cells to promote metastasis. Nat. Cell Biol. 16 (992-1003), 1001–1015.
Li, H., Song, F., Duan, L.R., Sheng, J.J., Xie, Y.H., Yang, Q., Chen, Y., Dong, Q.Q., Zhang, B.L., Wang, S.W., 2016. Paeonol and danshensu combination attenuates apoptosis in myocardial infarcted rats by inhibiting oxidative stress: roles of Nrf2/HO-1 and PI3K/Akt pathway. Sci. Rep. 6, 23693.
Liu, M.H., Lin, A.H., Ko, H.K., Perng, D.W., Lee, T.S., Kou, Y.R., 2017. Prevention of bleomycin-induced pulmonary inflammation and fibrosis in mice by paeonol. Front. Physiol. 8, 193.
Liu, M.H., Lin, A.H., Lee, H.F., Ko, H.K., Lee, T.S., Kou, Y.R., 2014. Paeonol attenuates cigarette smoke-induced lung inflammation by inhibiting ROS-sensitive inflammatory signaling. Med. Inflamm. 2014, 651890.
Lu, L., Qin, Y., Chen, C., Guo, X., 2018. Beneficial effects exerted by paeonol in the management of atherosclerosis. Oxid. Med. Cell. Longev. 2018, 1098617.
Luo, C., Widlund, H.R., Puigserver, P., 2016. PGC-1 coactivators: shepherding the mitochondrial biogenesis of tumors. Trends Cancer 2, 619–631.
Luo, X., Liao, C., Quan, J., Cheng, C., Zhao, X., Bode, A.M., Cao, Y., 2019. Posttranslational regulation of PGC-1alpha and its implication in cancer metabolism. Int. J. Cancer.
Ma, C., Zhang, C., Ma, M., Zhang, L., Zhang, L., Zhang, F., Chen, Y., Cao, F., Li, M., Wang, G., Shen, T., Yao, H., Liu, Y., Pan, Z., Song, S., Zhu, D., 2017. MiR-125a regulates mitochondrial homeostasis through targeting mitofusin 1 to control hypoxic pulmonary vascular remodeling. J. Mol. Med. 95, 977–993.
Marsboom, G., Toth, P.T., Ryan, J.J., Hong, Z., Wu, X., Fang, Y.H., Thenappan, T., Piao, L., Zhang, H.J., Pogoriler, J., Chen, Y., Morrow, E., Weir, E.K., Rehman, J., Archer, S.L., 2012. Dynamin-related protein 1-mediated mitochondrial mitotic fission permits hyperproliferation of vascular smooth muscle cells and offers a novel therapeutic target in pulmonary hypertension. Circ. Res. 110, 1484–1497.
Naoi, M., Wu, Y., Shamoto-Nagai, M., Maruyama, W., 2019. Mitochondria in neuroprotection by phytochemicals: bioactive polyphenols modulate mitochondrial apoptosis system, function and structure. Int. J. Mol. Sci. 20.
Nierenberg, A.A., Ghaznavi, S.A., Sande Mathias, I., Ellard, K.K., Janos, J.A., Sylvia, L.G., 2018. Peroxisome proliferator-activated receptor gamma Coactivator-1 alpha as a novel target for bipolar disorder and other neuropsychiatric disorders. Biol. Psychiatry 83, 761–769.
Onishi, Y., Ueha, T., Kawamoto, T., Hara, H., Toda, M., Harada, R., Minoda, M., Kurosaka, M., Akisue, T., 2014. Regulation of mitochondrial proliferation by PGC-1alpha induces cellular apoptosis in musculoskeletal malignancies. Sci. Rep. 4, 3916.
Picard, M., Wallace, D.C., Burelle, Y., 2016. The rise of mitochondria in medicine. Mitochondrion 30, 105–116.
Piccinin, E., Peres, C., Bellafante, E., Ducheix, S., Pinto, C., Villani, G., Moschetta, A., 2018. Hepatic peroxisome proliferator-activated receptor gamma coactivator 1beta drives mitochondrial and anabolic signatures that contribute to hepatocellular carcinoma progression in mice. Hepatology 67, 884–898.
Ryan, J.J., Marsboom, G., Fang, Y.H., Toth, P.T., Morrow, E., Luo, N., Piao, L., Hong, Z., Ericson, K., Zhang, H.J., Han, M., Haney, C.R., Chen, C.T., Sharp, W.W., Archer, S.L., 2013. PGC1alpha-mediated mitofusin-2 deficiency in female rats and humans with pulmonary arterial hypertension. Am. J. Respir. Crit. Care Med. 187, 865–878.
Sawada, N., Jiang, A., Takizawa, F., Safdar, A., Manika, A., Tesmenitsky, Y., Kang, K.T., Bischoff, J., Kalwa, H., Sartoretto, J.L., Kamei, Y., Benjamin, L.E., Watada, H., Ogawa, Y., Higashikuni, Y., Kessinger, C.W., Jaffer, F.A., Michel, T., Sata, M., Croce, K., Tanaka, R., Arany, Z., 2014. Endothelial PGC-1alpha mediates vascular dysfunction in diabetes. Cell Metab. 19, 246–258.
Wang, J.L., Chen, C.W., Tsai, M.R., Liu, S.F., Hung, T.J., Yu Ju, H., Chang, W.T., Shi, M.D., Hsieh, P.F., Yang, Y.L., 2018. Antifibrotic role of PGC-1alpha-siRNA against TGF-beta1-induced renal interstitial fibrosis. Exp. Cell Res. 370, 160–167.
Ye, J.X., Wang, S.S., Ge, M., Wang, D.J., 2016. Suppression of endothelial PGC-1alpha is associated with hypoxia-induced endothelial dysfunction and provides a new therapeutic target in pulmonary arterial hypertension. Am. J. Physiol. Lung Cell Mol. Physiol. 310, L1233–L1242.
Zhang, L., Ma, C., Gu, R., Zhang, M., Wang, X., Yang, L., Liu, Y., Zhou, Y., He, S., Zhu, D., 2018. Paeonol regulates hypoxia-induced proliferation of pulmonary artery smooth muscle cells via EKR 1/2 signalling. Eur. J. Pharmacol. 834, 257–265.
Zhang, L., Ma, C., Zhang, C., Ma, M., Zhang, F., Zhang, L., Chen, Y., Cao, F., Li, S., Zhu, D., 2016. Reactive oxygen species effect PASMCs apoptosis via regulation of dynamin-related protein 1 in hypoxic pulmonary hypertension. Histochem. Cell Biol. 146, 71–84.
Zhang, Y., Wang, M., Xu, X., Liu, Y., Xiao, C., 2019. Matrine promotes apoptosis in SW480 colorectal cancer cells via elevating MIEF1-related mitochondrial division in a manner dependent on LATS2-Hippo pathway. J. Cell. Physiol.
Zhu, L., Sun, G., Zhang, H., Zhang, Y., Chen, X., Jiang, X., Jiang, X., Krauss, S., Zhang, J., Xiang, Y., Zhang, C.Y., 2009. PGC-1alpha is a key regulator of glucose-induced proliferation and migration in vascular smooth muscle cells. PLoS One 4, e4182.